

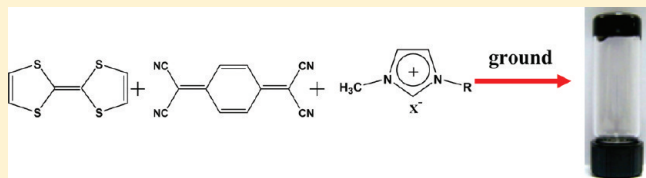
Electronically and Ionically Conductive Gels of Ionic Liquids and Charge-Transfer Tetrathiafulvalene–Tetracyanoquinodimethane

Xiaoguang Mei and Jianyong Ouyang*

Department of Materials Science and Engineering, National University of Singapore, Singapore 117576

Supporting Information

ABSTRACT: Electronically and ionically conductive gels were fabricated by mixing and mechanically grinding neutral tetrathiafulvalene (TTF) and tetracyanoquinodimethane (TCNQ) in ionic liquids (ILs) like 3-ethyl-1-methylimidazolium dicyanoamide (EMIDCA), 1-ethyl-3-methylimidazolium thiocyanate (EMISCN), 1-ethyl-3-methylimidazolium bis(trifluoromethylsulfonyl)imide (EMITf₂N), trihexyltetradecylphosphonium bis(trifluoromethylsulfonyl)imide (P_{14,6,6,6}Tf₂N), and methyl-trioctylammonium bis(trifluoromethylsulfonyl)imide (MOATf₂N). Charge-transfer TTF–TCNQ crystallites were generated during the mechanical grinding as indicated by the UV–visible–near-infrared (UV–vis–NIR) absorption spectroscopy, Fourier transform infrared (FTIR) spectroscopy, and X-ray diffraction. The charge-transfer TTF–TCNQ crystallites have a needle-like shape. They form solid networks to gelate the ILs. The gel behavior is confirmed by the dynamic mechanical measurements. It depends on both the anions and cations of the ILs. In addition, when 1-methyl-3-butylimidazolium tetrafluoroborate (BMIBF₄) and 1-methyl-3-propylimidazolium iodide (PMII) were used, the TTF–TCNQ/IL mixtures did not behave as gels. The TTF–TCNQ/IL gels are both electronically and ionically conductive, because the solid phase formed by the charge-transfer TTF–TCNQ crystallites is electronically conductive, while the ILs are ionically conductive. The gel formation is related to needle-like charge-transfer TTF–TCNQ crystallites and the π – π and Coulombic interactions between TTF–TCNQ and ILs.



1. INTRODUCTION

Physical gels, in which the gelators do not chemically bond together, have been attracting considerable interest due to their unique architecture and diverse potential applications.¹ Various small molecules from simple alkanes to complex phthalocyanines, can function as the gelators for water or organic solvents. These molecules usually have a rigid unit and a soft tail. They assemble into three-dimensional (3D) fibrous networks as the result of the interaction among the rigid structure of molecules. They can immobilize liquids by noncovalent interactions, such as hydrogen bonding and van der Waals interaction. Recently, conductive gels were demonstrated and gained strong attention. The conductivity can originate from the solid networks or the fluid in the gels. Two types of conductive materials have been used to gelate organic liquids. Conjugated molecules, particularly organic donors and acceptors, can have high conductivity when in the oxidized or reduced state. Several groups have reported gels with derivatives of an organic donor, tetrathiafulvalene (TTF), as the gellator.² These gels become electronically conductive when the TTF unit is oxidized. Kitamura et al. observed a conductivity of 10^{−5} S/cm for gels of a TTF derivative doped with tetracyanoquinomethane (TCNQ). Another type of conductive material is carbon nanotubes. Both pristine and chemically functionalized carbon nanotubes have been used to gelate organic solvents and other organic liquids.³ On the other hand, ionically conductive gels were demonstrated as well by using ionic liquids (ILs) as the fluid in gels. ILs can form gels with

many different materials, including polymers,⁴ small organic molecules,⁵ nanoparticles,⁶ and carbon nanotubes.⁷ Their gels can have many unique applications due to the advantages of ILs in comparison with water and normal organic solvents.⁸ For example, they can be used as stable electrolytes in energy-related devices, such as dye-sensitized solar cells,⁹ secondary batteries,¹⁰ electrochromic displays,¹¹ and supercapacitors.¹² These gels have solid-like appearance and high ionic conductivity. Carbon nanotube/IL gels have both electronic and ionic conductivities.⁷ The carbon nanotubes form solid networks, which are mediated by the van der Waals force or the cation– π interaction between carbon nanotubes and ILs, and provide electronic conductivity for the gels.

Here, we report novel gels with both electronic and ionic conductivities, which are formed by ILs and charge-transfer TTF–TCNQ. TTF and TCNQ, whose chemical structures are shown in Figure 1(a), are chosen because they are a popular organic donor and acceptor, respectively. Charge transfer can take place between TTF and TCNQ, when their solutions are mixed together.¹³ The solution mixing results into charge-transfer TTF–TCNQ crystallites, which usually have a needle-like shape. They are highly conductive along the molecule stacking direction.¹⁴ In fact, TTF–TCNQ is the first metallic

Received: January 3, 2011

Revised: July 29, 2011

Published: July 29, 2011

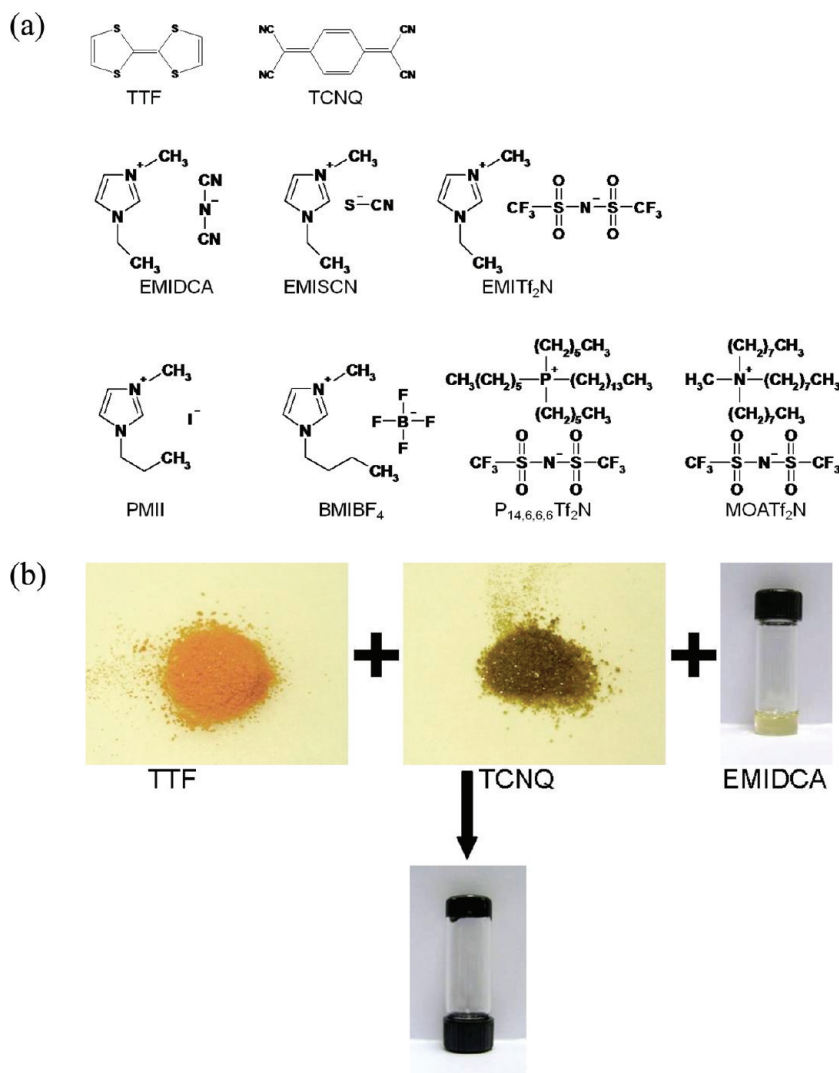


Figure 1. (a) Chemical structures of TTF, TCNQ, EMIDCA, BMIBF₄, EMISCN, PMII, EMITf₂N, P_{14,6,6,6}Tf₂N, and MOATf₂N. (b) Photographs of TTF, TCNQ, EMIDCA, and a gel of TTF–TCNQ/EMIDCA.

organic charge-transfer complex. However, no gel formation has been reported with unmodified TTF or TCNQ as the gelator. We found that TTF and TCNQ can form gels with ILs through a process similar to the preparation of gels of carbon nanotubes and ILs.⁷

2. EXPERIMENTAL SECTION

2.1. Materials. All the chemicals, including TTF, TCNQ, 3-ethyl-1-methylimidazolium dicyanamide (EMIDCA), 1-ethyl-3-methylimidazolium thiocyanate (EMISCN), 1-ethyl-3-methylimidazolium bis(trifluoromethylsulfonyl)imide (EMITf₂N), 1-methyl-3-propylimidazolium iodide (PMII), 1-methyl-3-butylimidazolium tetrafluoroborate (BMIBF₄), trihexyltetradecylphosphonium bis(trifluoromethylsulfonyl)imide (P_{14,6,6,6}Tf₂N) and methyl-trioctylammonium bis(trifluoromethylsulfonyl)imide (MOATf₂N), were purchased from Sigma-Aldrich and used without further purification. Figure 1a presents the chemical structures of TTF, TCNQ, and these ILs.

2.2. Gel Preparation. The TTF–TCNQ/IL gels were prepared by mechanically grinding neutral TTF and TCNQ in ILs. Equimolar (or equiweight) TTF and TCNQ were used in all the experiments. Since

TTF and TCNQ have almost the same molecular weight, their weight ratio approximately equals their molar ratio. In a typical experiment, 50 mg TTF and 50 mg TCNQ were mixed and ground in an agate mortar for 5 min. IL (400 mg) was then added into the mortar, and the mixture was further ground for 5 min. Xerogels of TTF–TCNQ were prepared by rinsing TTF–TCNQ/IL gels with ethanol for 10 min. The rinse was repeated several times to remove the ILs. Then, the TTF–TCNQ was dried in air at room temperature.

2.3. Characterization. The rheological properties of the gels were measured with a Rheometric Scientific Advanced Rheometric Expansion System (ARES) in the dynamic mode with cone-to-plate configuration. The diameter of the cone was 2.5 cm, and the cone angle was 0.04 rad. The gap between cone and plate was 0.5 mm. Scanning electron microscopic (SEM) images were taken with a Hitachi S-4100 scanning electron microscope. The conductivity of the gels was measured by the dc four-point probe technique with a Keithley 2400 source/meter. The measurement was performed by placing a gel on a glass slide attached with four copper foils, which served as the four probes. The thickness of the gel was controlled by placing another glass substrate on the top of the gel. The UV–visible–near-infrared (UV–vis–NIR) absorption spectra were recorded with a Varian Cary 5000 UV–vis–NIR Spectrometer. The TTF (or TCNQ) samples were prepared by drop casting and drying

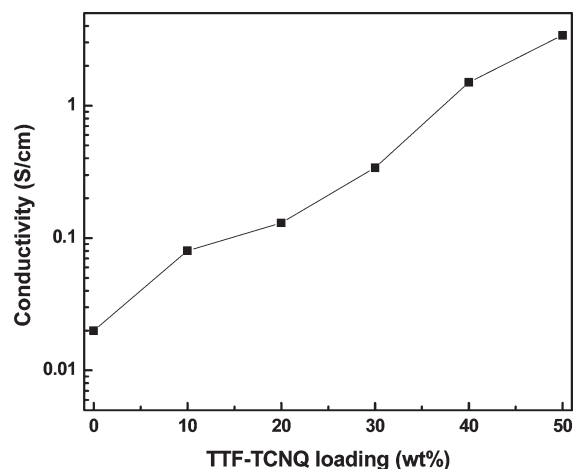


Figure 2. Variation of the conductivity of TTF–TCNQ/EMIDCA gels with the TTF–TCNQ loading. The molar ratio of TTF to TCNQ was kept as 1:1.

acetonitrile solution of TTF (or TCNQ) onto quartz substrates. The TTF–TCNQ/IL samples were prepared by coating thin gel layers onto quartz substrates by the doctor blade method. The FTIR spectra were acquired using a Varian 3100 FT-IR spectrometer. The X-ray diffraction (XRD) patterns were measured with a Bruker Bragg–Brentano theta X-ray diffractometer.

3. RESULTS AND DISCUSSION

3.1. TTF–TCNQ/EMIDCA Gels. EMIDCA is a fluid at room temperature. After EMIDCA was ground with neutral TTF and TCNQ for a few minutes, the mixture could not flow and turned into a black gel. Figure 1b illustrates this process. Equimolar (or equiweight) TTF and TCNQ were always used to follow the 1:1 molar ratio between TTF and TCNQ in the charge-transfer TTF–TCNQ complex. In a typical experiment, 50 mg TTF and 50 mg TCNQ was mixed by mechanical grinding for 5 min. The mixture was then ground with 400 mg EMIDCA for another 5 min. TTF–TCNQ/EMIDCA is used to represent this gel. The properties of the TTF–TCNQ/EMIDCA gels depend on the loading of TTF and TCNQ. When more TTF and TCNQ were used, the gels became more solid-like. The mixtures of TTF, TCNQ, and EMIDCA behaved as gels even when the loading of TTF and TCNQ was reduced to 10 wt %.

The TTF–TCNQ/EMIDCA gel is electrically conductive. Its conductivity almost linearly increases with increasing TTF–TCNQ loading (Figure 2). Pure EMIDCA had a conductivity of 0.02 S/cm, which arises from the ion transport under an external electric field. The conductivity increased by about 1 order in magnitude to 10^{-1} S/cm for the TTF–TCNQ/EMIDCA gel with 10 wt % TTF–TCNQ. It was further increased to 3.8 S cm^{-1} , when the TTF–TCNQ loading was increased to 50 wt %. The higher conductivity of the gels in comparison with pure EMIDCA suggests that the TTF–TCNQ/EMIDCA gels are also electronically conductive. The electronic conductivity is due to neither neutral TTF nor TCNQ, because both of them are insulators, and a TTF/EMIDCA or TCNQ/EMIDCA mixture has almost the same conductivity as pure EMIDCA. Thus, it should arise from the product of TTF and TCNQ during the mechanical grinding in EMIDCA.

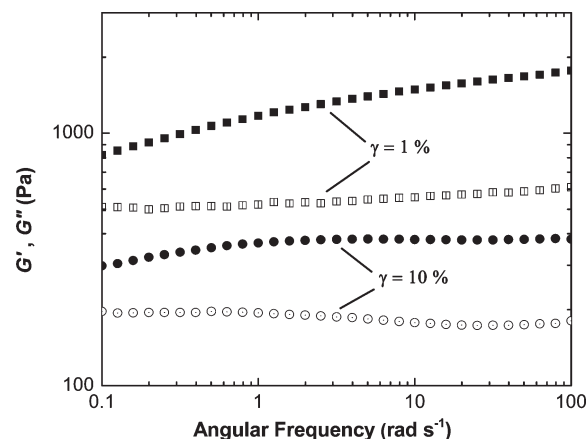


Figure 3. Angular frequency dependencies of dynamic storage (G' , solid symbols) and loss moduli (G'' , open symbols) of a TTF–TCNQ/EMIDCA gel at 25 °C. Applied strain amplitudes (γ) were 1% (squares) and 10% (circles). The loading of TTF–TCNQ is 20 wt % in the gel.

The gel behavior of the TTF–TCNQ/EMIDCA mixtures was confirmed by dynamic mechanical measurements. Figure 3 shows the dependencies of the storage (G') and loss (G'') moduli of a TTF–TCNQ/EMIDCA gel on the angular frequency at a strain of 1%. G' has a weak dependence on the angular frequency, while G'' is almost flat. Since the magnitude of G' is much higher than that of G'' , the mechanical properties of the mixture are dominated by the solid phase rather than the liquid phase. These results indicate the existence of 3D solid networks in the gel. The solid network in the gel is quite stable under distortion. No sign of yielding was observed even when the shear strain was increased to 10%. The formation of these TTF–TCNQ/IL gels may be similar to the nanoparticle/IL⁶ and carbon nanotube/IL⁷ gels, while different from low-mass organogels that are usually formed by a sol–gel process.¹

There should be at least two phases, a solid phase and a liquid phase, in the TTF–TCNQ/IL gels. The microstructure of the TTF–TCNQ/IL gels was studied by SEM. Figure 4a shows the SEM image of a TTF–TCNQ/EMIDCA gel with 50 wt % of TTF–TCNQ. The solid phase is needle-like crystallites, which have a diameter of about 100 nm and a length of 1–2 μm . The solid networks were clearly observed in the TTF–TCNQ xerogel, which was prepared by washing away EMIDCA with ethanol from the TTF–TCNQ/EMIDCA gel (Figure 4b). It is worth noting that the solid networks are formed by neither neutral TTF nor neutral TCNQ. Neutral TTF or TCNQ alone does not form a gel with EMIDCA.

We also mixed equimolar TTF and TCNQ in acetonitrile in terms of the literature.^{13b} TTF and TCNQ did not form a gel with acetonitrile. Instead, charge-transfer TTF–TCNQ crystallites were obtained (Figure 4c). They are larger and longer than the TTF–TCNQ crystallites formed in the gels.

The needle-like crystallites observed in the SEM image of the TTF–TCNQ/EMIDCA gel are neither neutral TTF nor TCNQ. The UV–vis–NIR absorption of the TTF–TCNQ/EMIDCA gel is significantly different from that of neutral TTF and TCNQ (Figure 5). The two absorption bands between 800 and 1100 nm for the TTF–TCNQ/EMIDCA gel are due to the TCNQ radical anions.¹⁵ The broad absorption of the TTF–TCNQ/EMIDCA gel in the infrared range can be attributed to the plasmonic absorption of the charge-transfer

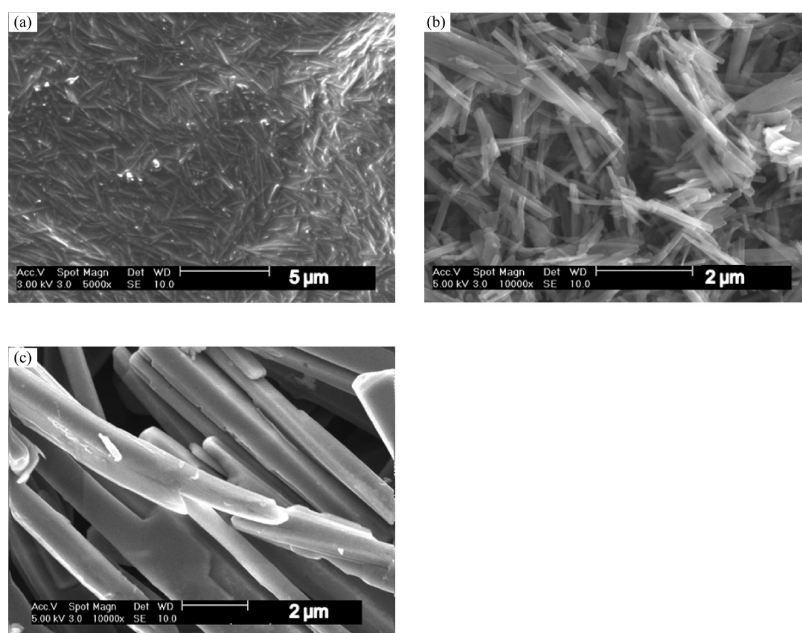


Figure 4. SEM images of (a) TTF-TCNQ/EMIDCA gel with 50 wt % of TTF and TCNQ, (b) TTF-TCNQ xerogel prepared by washing away EMIDCA from the TTF-TCNQ/EMIDCA gel, and (c) TTF-TCNQ complex prepared by mixing acetonitrile solutions of equimolar TTF and TCNQ.

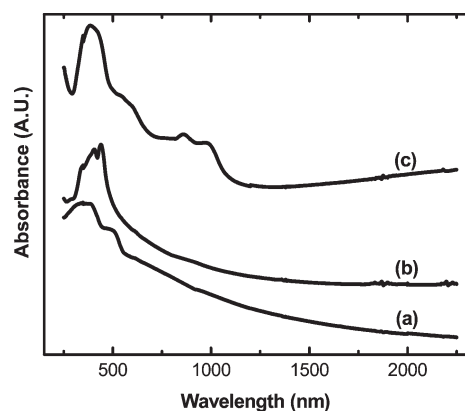
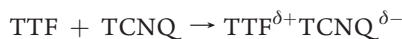


Figure 5. UV-vis-NIR absorption of (a) TTF, (b) TCNQ, and (c) TTF-TCNQ/EMIDCA gel. The weight loading of TTF and TCNQ was 50 wt % in the gel.

TTF-TCNQ.¹⁶ The charge-transfer TTF-TCNQ complex is formed during the mechanical grinding of neutral TTF and TCNQ:



δ is 0.59, if we assume that it is the same as that in the charge-transfer TTF-TCNQ complex by solution mixing.¹⁶

The charge-transfer TTF-TCNQ in the gels is further supported by the FTIR spectra of TTF, TCNQ, EMIDCA, and TTF-TCNQ/EMIDCA gel (Figure 6). The FTIR spectrum of TTF-TCNQ complex prepared by mixing the acetonitrile solutions of TTF and TCNQ is shown as well. The FTIR of the TTF-TCNQ/EMIDCA gel is quite similar to that of TTF-TCNQ complex by solution mixing. Some additional vibrational bands observed for the former can be attributed to EMIDCA. But the FTIR of TTF-TCNQ/EMIDCA gel is quite

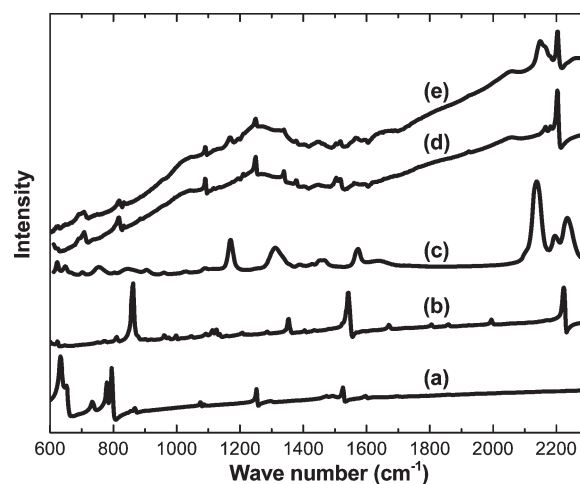


Figure 6. FTIR of (a) TTF, (b) TCNQ, (c) EMIDCA, (d) TTF-TCNQ complex, and (e) TTF-TCNQ/EMIDCA gel. The TTF-TCNQ complex was prepared by mixing acetonitrile solutions of TTF and TCNQ at 1:1 molar ratio. The loading of TTF and TCNQ was 50 wt % in the gel.

different from that of neutral TTF and neutral TCNQ. The vibrational band at 1525 cm^{-1} for neutral TTF corresponds to the C=C stretching.¹⁷ This vibrational band shifts to 1562 cm^{-1} for the TTF-TCNQ/EMIDCA gel and the TTF-TCNQ complex by solution mixing. The blue shift in the C=C stretching band evidences that TTF is positively charged in the gel.¹⁸ Shift in a vibrational band was also observed for TCNQ. The vibrational band at 2224 cm^{-1} is due to the C≡N stretching of neutral TCNQ.¹⁹ This vibration band shifts to 2204 cm^{-1} for TTF-TCNQ/EMIDCA gel and TTF-TCNQ complex by solution mixing. The red shift confirms that TCNQ is negatively charged in the TTF-TCNQ/EMIDCA gel.

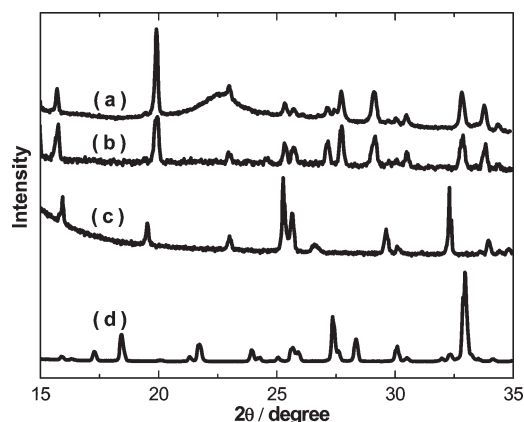


Figure 7. XRD patterns of (a) TTF–TCNQ/EMIDCA gel, (b) TTF–TCNQ complex, (c) TTF, and (d) TCNQ. The TTF–TCNQ complex was prepared by mixing acetonitrile solutions of TTF and TCNQ at 1:1 molar ratio. The loading of TTF and TCNQ was 50 wt % in the gel.

Although both neutral TTF and TCNQ have a poor solubility in EMIDCA, they can form a charge-transfer complex in EMIDCA. Charge transfer between TTF and TCNQ even in solid state was observed at the interface of TTF and TCNQ crystals by Alves et al.²⁰ and a mixture of TTF and TCNQ by thermal deposition.²¹ The formation of charge-transfer TTF–TCNQ crystallites in the gels is consistent with the XRD patterns. Figure 7 shows the XRD patterns of a TTF–TCNQ/EMIDCA gel, TTF, TCNQ, and TTF–TCNQ complex by solution mixing. Several XRD bands were observed for the TTF–TCNQ/EMIDCA gel. They appear at the same angles as those of the TTF–TCNQ complex by solution mixing, but significantly different from those of neutral TTF and TCNQ. The XRD patterns also evidence that the solid phase in the TTF–TCNQ/EMIDCA gel is crystallites of charge-transfer TTF–TCNQ.^{21a,22} Presumably, these charge-transfer TTF–TCNQ crystallites are related to the diffusion of neutral TTF and TCNQ molecules in EMIDCA and growth of charge-transfer TTF–TCNQ crystallites. Both neutral TTF and TCNQ have a poor solubility in EMIDCA, so that small amount of neutral TTF and TCNQ molecules is present in EMIDCA. These neutral TTF and TCNQ molecules can diffuse in the relatively less viscous EMIDCA and form charge-transfer TTF–TCNQ complex.

TTF and TCNQ are conjugated molecules. They have positive and negative charges, respectively, in charge-transfer TTF–TCNQ. Presumably, the gel formation of TTF–TCNQ with EMIDCA is related to the one-dimensional TTF–TCNQ crystallites and the interactions between TTF–TCNQ and EMIDCA. There are π – π and Coulombic interactions between charge-transfer TTF–TCNQ and EMIDCA. The π – π interaction between TTF–TCNQ crystallites and EMIDCA may be similar to that between carbon nanotubes and ILs, while there are additional Coulombic interactions between TTF–TCNQ and EMIDCA. In terms of this mechanism for the gel formation, TTF–TCNQ/EMIDCA gels can be formed by grinding charge-transfer TTF–TCNQ complex, which is prepared by solution mixing, in EMIDCA. We did observe it. But the conductivity of a gel formed by grinding 50 wt % TTF–TCNQ complex by solution mixing with 50 wt % EMIDCA was only 1.2 S/cm, lower than that (3.8 S/cm) formed by grinding neutral TTF and TCNQ with EMIDCA. These results imply that TTF–TCNQ

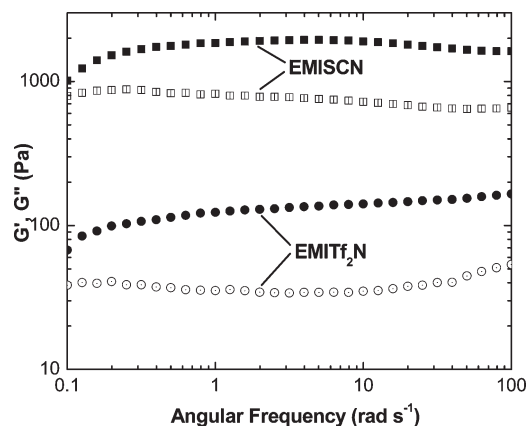


Figure 8. Angular frequency dependencies of G' (solid symbols) and G'' (open symbols) of TTF–TCNQ/EMISCN (squares) and TTF–TCNQ/EMITf₂N (circles) gels at 25 °C. Applied strain amplitude (γ) was 1%. The loading of TTF and TCNQ was 20 wt % in the gels.

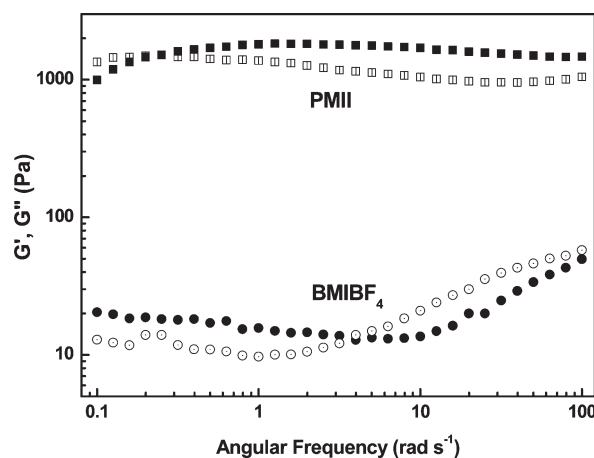


Figure 9. Angular frequency dependencies of G' (solid symbols) and G'' (open symbols) of TTF–TCNQ/PMII (squares) and TTF–TCNQ/BMIBF₄ (circles) mixtures at 25 °C. Applied strain amplitude (γ) was 1%. The loading of TTF and TCNQ was 20 wt % in the mixtures.

crystallites grown during the mechanical grinding of neutral TTF and TCNQ in EMIDCA can form more effective solid networks than directly grinding TTF–TCNQ complex prepared by solution mixing in EMIDCA. The possible reason is the smaller TTF–TCNQ crystallites formed by grinding neutral TTF and TCNQ in EMIDCA as observed by SEM in Figure 4.

The formation mechanism of the TTF–TCNQ/EMIDCA gels is different from that for organogels with organic donor (or acceptor) derivatives or complexes.^{2,23} The organic donor (or acceptor) derivatives usually have a donor (or acceptor) unit together with a long alkyl tail. The gel formation mechanism is attributed to the van der Waals forces among donor (or acceptor) units and the van der Waals forces between the alkyl tails and solvent.

3.2. Effect of ILs on TTF–TCNQ/IL Gels. As mentioned above, the gel formation is related to the TTF–TCNQ crystallites grown during the grinding and the interactions between charge-transfer TTF–TCNQ and ILs. They should depend on

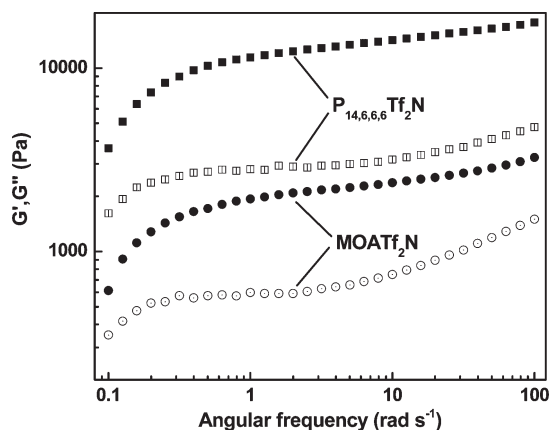


Figure 10. Angular frequency dependencies of G' (solid symbols) and G'' (open symbols) of (a) TTF–TCNQ/ $P_{14,6,6,6}Tf_2N$ (squares) and TTF–TCNQ/MOATf₂N (circles) mixtures at 25 °C. Applied strain amplitude (γ) was 1%. The loading of TTF and TCNQ was 20 wt % in the gels.

both the cations and anions of ILs.²⁴ Besides EMIDCA, TTF and TCNQ were also mixed and mechanically ground in other ILs in order to understand the effect of ILs on the formation, structure, and properties of TTF–TCNQ/IL gels. As shown in Figure 1a, two ILs, EMISCN and EMITf₂N, have the same cation as EMIDCA. They were chosen to study the effect of the anion on the TTF–TCNQ/IL gels. The dynamic mechanical measurements of TTF–TCNQ/EMISCN and TTF–TCNQ/EMITf₂N are shown in Figure 8. These results indicate that both TTF–TCNQ/EMISCN and TTF–TCNQ/EMITf₂N are gels. But the anions affect the G' and G'' values. The G' and G'' values of TTF–TCNQ/EMISCN are not too different from that of TTF–TCNQ/EMIDCA, whereas they are saliently higher than that of TTF–TCNQ/EMITf₂N; that is, TTF–TCNQ/EMISCN and TTF–TCNQ/EMIDCA are stronger gels than TTF–TCNQ/EMITf₂N. This difference is probably related to the bulky anion of EMITf₂N.

We also investigated TTF–TCNQ gels with imidazole ILs of different side chains, because the side chain of imidazole can significantly affect the properties of ILs.²⁵ Figure 9 shows the dynamical mechanical results of TTF–TCNQ/PMII and TTF–TCNQ/BMIBF₄. The G' value of TTF–TCNQ/PMII is even lower than G'' at the low frequency range. The G' value surpasses G'' at $\omega = 0.3$ rad/s. However, the difference between G' and G'' is not significant in the whole frequency range. Thus, TTF–TCNQ/PMII is a very weak gel or cannot be considered as a gel. The dynamical mechanical behavior of TTF–TCNQ/BMIBF₄ becomes quite different from a gel. G'' is higher than G' at the high frequency range. TTF–TCNQ/BMIBF₄ is thus not a gel. A mixture other than gel is used to describe TTF–TCNQ/PMII and TTF–TCNQ/BMIBF₄. The cations of EMIDCA, PMII, and BMIBF₄ have side alkyl chains of different lengths. The side alkyl chain may affect the interactions between the conjugated imidazole unit and TTF–TCNQ, including both the π – π and Coulombic interactions, which contribute to different mechanical behaviors of the TTF–TCNQ/IL gels or mixtures.

In order to understand whether the π – π interaction or the Coulombic interaction between TTF–TCNQ and ILs is more important, ILs, $P_{14,6,6,6}Tf_2N$ and MOATf₂N, were used to prepare TTF–TCNQ/IL gels. The cations of these two ILs do

not have any conjugated structure, while their anions are the same as that of EMITf₂N. The dynamic measurements suggest that both TTF–TCNQ/ $P_{14,6,6,6}Tf_2N$ and TTF–TCNQ/MOATf₂N are gels (Figure 10). Probably, the Coulombic interaction between the ILs and TTF–TCNQ is the major factor for the gel formation, at least for these two gels.

The effect of the ILs on the formation and properties of TTF–TCNQ/IL gels can be understood in terms of the shape of the charge-transfer TTF–TCNQ crystallites formed in these ILs. Figure 11 presents the SEM images of the TTF–TCNQ xerogels prepared from the TTF–TCNQ/IL gels or mixtures. It is more convenient to understand the different behaviors of TTF–TCNQ/IL mixtures in terms of these SEM images than that of TTF–TCNQ/IL gels or mixtures (Figure S1 in the Supporting Information). TTF–TCNQ crystallites obtained from TTF–TCNQ/BMIBF₄ are short and wide (Figure 11d), while those obtained from TTF–TCNQ/EMISCN are remarkably longer and narrower (Figure 11a). The long and narrow structure is favorable for the formation of 3D solid-state networks. These account for the different mechanical behaviors of TTF–TCNQ/BMIBF₄ and TTF–TCNQ/EMISCN. TTF–TCNQ crystallites obtained from TTF–TCNQ/EMITf₂N (Figure 11b) are also remarkably shorter and wider than that from TTF–TCNQ/EMIDCA (Figure 4b). Thus, TTF–TCNQ/EMITf₂N has much lower mechanical moduli (lower G' and G'') than TTF–TCNQ/EMIDCA. The gel behavior of TTF–TCNQ with the nonconjugated ILs, $P_{14,6,6,6}Tf_2N$ (Figure 11e) and MOATf₂N (Figure 11f), can be understood according to their SEM images as well. The quite narrow TTF–TCNQ crystallites enable the formation of TTF–TCNQ solid networks in these ILs.

Charge-transfer TTF–TCNQ is formed after mechanically grinding neutral TTF and TCNQ in those ILs as evidenced by the UV–vis–NIR absorption spectra, FTIR spectra, and XRD patterns (Figures S2, S3, and S4 in the Supporting Information). The FTIR spectra and XRD patterns also indicate that the ILs can affect the formation of the charge-transfer TTF–TCNQ during the mechanical grinding of neutral TTF and TCNQ. The diffraction peaks of neutral TTF and TCNQ can be observed in the XRD patterns of TTF–TCNQ/ $P_{14,6,6,6}Tf_2N$ and TTF–TCNQ/MOATf₂N. This may be related to the very poor solubility of neutral TTF and TCNQ in these two ILs and the high viscosity of these ILs. The solubility of neutral TTF and TCNQ is poorer in nonconjugated ILs than the conjugated ILs due to the absence of the π – π interaction for the former. $P_{14,6,6,6}Tf_2N$ and MOATf₂N have a high viscosity, which makes the diffusion of TTF and TCNQ difficult. Probably, charge-transfer TTF–TCNQ encapsulates some neutral TTF (or TCNQ) molecules and prevents them from contacting neutral TCNQ (or TTF).

The gel formation includes the following steps: (1) diffusion of neutral TTF and TCNQ molecules in ILs; (2) formation of charge-transfer TTF–TCNQ in ILs, (3) growth of charge-transfer TTF–TCNQ crystallites, and (4) formation of solid networks by the TTF–TCNQ crystallites. Steps 1–3 result in the TTF–TCNQ crystallites in ILs. ILs affect all four steps. The first step depends on the interaction between ILs and neutral TTF and TCNQ and the viscosity of ILs. EMIDCA, EMISCN, EMITf₂N, and BMIBF₄ have a lower viscosity, while PMII has a viscosity higher than that of $P_{14,6,6,6}Tf_2N$ and MOATf₂N.²⁶ However, the TTF–TCNQ crystallites grown in PMII are large, whereas they are small in the nonconjugated $P_{14,6,6,6}Tf_2N$ and

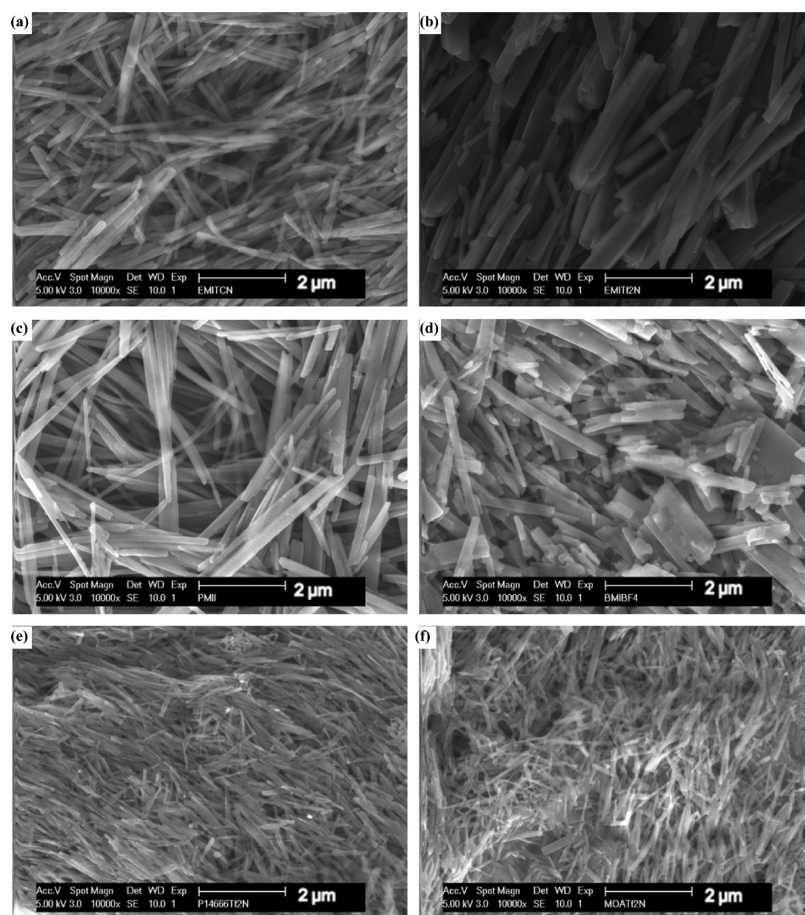


Figure 11. SEM images of TTF–TCNQ xerogels prepared from (a) TTF–TCNQ/EMISCN, (b) TTF–TCNQ/EMITf₂N, (c) TTF–TCNQ/PMII, (d) TTF–TCNQ/BMIBF₄, (e) TTF–TCNQ/P_{14,6,6,6}Tf₂N, and (f) TTF–TCNQ/MOATf₂N mixtures. The loading of TTF–TCNQ in the mixtures was 50 wt %. The xerogels were prepared by washing away the ILs from the TTF–TCNQ/IL mixtures.

MOATf₂N. Therefore, the π – π interaction between ILs and neutral TTF and TCNQ may be the dominant factor for the growth of TTF–TCNQ crystallites in ILs. Nonconjugated P_{14,6,6,6}Tf₂N and MOATf₂N have weak interaction with neutral TTF and TCNQ. Consequently, the first step is slow, and there are more neutral TTF and TCNQ in the gels with the nonconjugated ILs than that with the conjugated ILs. The formation of the solid networks of TTF–TCNQ crystallites is mediated by the π – π and Coulombic interactions between TTF–TCNQ and ILs. However, the Coulombic interaction is much stronger than the π – π interaction and should be the major factor. Thus, TTF–TCNQ/IL mixtures with the nonconjugated ILs behave as a gel.

The gel formation is due to the formation of charge-transfer TTF–TCNQ solid networks in ILs. The solid networks in the gels should affect the conductivity of the TTF–TCNQ/IL gels or mixtures. The conductivities are 0.53, 0.43, and 0.47 S/cm for the gels or mixtures of 50 wt % TTF–TCNQ with 50 wt % EMITf₂N, P_{14,6,6,6}Tf₂N and MOATf₂N, respectively. They drop to 0.15, 0.05, and 0.07 S/cm for the mixtures of 50 wt % TTF–TCNQ with 50 wt % PMII, EMISCN, and BMIBF₄, respectively. These conductivities are generally consistent with the structure of these gels or mixtures. The conductivity is determined by the structure of the gels or mixtures other than the morphology of the TTF–TCNQ crystallites. For instance, although the morphology of TTF–TCNQ crystallites in

EMITf₂N is quite different from that in P_{14,6,6,6}Tf₂N and MOATf₂N, these gels exhibit similar high conductivities. When the TTF–TCNQ crystallites form continuous conductive solid networks in the ILs, the TTF–TCNQ/ILs behave as gels and can have high conductivity. However, if TTF–TCNQ crystallites cannot form a gel with an IL, there is no continuous conductive solid network in the TTF–TCNQ/IL mixture, giving rise to low conductivity.

Charge-transfer TTF–TCNQ complex is conductive. It can be used as an electrode in electronic devices.²⁷ The TTF–TCNQ gels developed in this work will enable the fabrication of conductive TTF–TCNQ through a gel process. This will be important for the application of charge-transfer TTF–TCNQ.

CONCLUSIONS

In conclusion, electronically and ionically conductive gels were prepared by mechanically grinding neutral TTF and TCNQ in ILs. Conductive charge-transfer TTF–TCNQ crystallites were generated during the mechanical grinding. They form solid networks to gelate ILs. These TTF–TCNQ/IL gels are electronically and ionically conductive, because the solid TTF–TCNQ phase is electronically conductive, while the ILs are ionically conductive. The gel formation is related to the TTF–TCNQ crystallites grown during the mechanical grinding and the π – π

and the Coulombic interactions between TTF–TCNQ and ILs. Both the cation and anion of ILs affect the structure and properties of the TTF–TCNQ/IL gels or mixtures. To the best of our knowledge, this is the first report on gels made of organic donor and acceptor without any chemical modification.

■ ASSOCIATED CONTENT

S Supporting Information. SEM images and UV-Vis-NIR and FTIR absorption spectra of TTF–TCNQ/EMSCN, TTF–TCNQ/EMITf₂N, TTF–TCNQ/PMII, TTF–TCNQ/BMIBF₄, TTF–TCNQ/P_{14,6,6}Tf₂N, and TTF–TCNQ/MOATf₂N mixtures, as well as XRDs of TTF–TCNQ/IL mixtures. This material is available free of charge via the Internet at <http://pubs.acs.org>.

■ AUTHOR INFORMATION

Corresponding Author

*E-mail: mseoj@nus.edu.sg.

■ ACKNOWLEDGMENT

This study was supported by a grant from the Ministry of Education, Singapore (R-284-000-086-112).

■ REFERENCES

- (1) (a) Gansauer, A.; Winkler, I.; Klawonn, T.; Nolte, R. J. M.; Feiters, M. C.; Borner, H. G.; Hentschel, J.; Dotz, K. H. *Organometallics* **2009**, *28*, 1377. (b) Ajayaghosh, A.; Praveen, V. K.; Vijayakumar, C. *Chem. Soc. Rev.* **2008**, *37*, 109.
- (2) (a) Kitahara, T.; Shirakawa, M.; Kawano, S.; Beginn, U.; Fujita, N.; Shinkai, S. *J. Am. Chem. Soc.* **2005**, *127*, 14980. (b) Kitamura, T.; Nakaso, S.; Mizoshita, N.; Tochigi, Y.; Shimomura, T.; Moriyama, M.; Ito, K.; Kato, T. *J. Am. Chem. Soc.* **2005**, *127*, 14769. (c) Wang, C.; Zhang, D.; Zhu, D. *J. Am. Chem. Soc.* **2005**, *127*, 16372. (d) Wang, C.; Chen, Q.; Sun, F.; Zhang, D.; Zhang, G.; Huang, Y.; Zhao, R.; Zhu, D. *J. Am. Chem. Soc.* **2010**, *132*, 3092. (e) Akutagawa, T.; Kakiuchi, K.; Hasegawa, T.; Noro, S.; Nakamura, T.; Hasegawa, H.; Mashiko, S.; Becher, J. *Angew. Chem., Int. Ed.* **2005**, *44*, 7283. (f) Akutagawa, T.; Kakiuchi, K.; Hasegawa, T.; Nakamura, T.; Christensen, C. A.; Becher, J. *Langmuir* **2004**, *20*, 4187. (g) Maitra, U.; Kumar, P. V.; Chandra, N.; DSouza, L. J.; Prasanna, M. D.; Raju, A. R. *Chem. Commun.* **1999**, 595.
- (3) (a) Moniruzzaman, M.; Sahin, A.; Winey, K. I. *Carbon* **2009**, *47*, 645. (b) Chen, J.; Xue, C.; Ramasubramanian, R.; Liu, H. *Carbon* **2006**, *44*, 2142. (c) Mei, X.; Ouyang, J. *Carbon* **2010**, *48*, 293. (d) Mei, X.; Cho, S. J.; Fan, B.; Ouyang, J. *Nanotechnology* **2010**, *21*, 395202.
- (4) (a) Lu, J.; Yan, F.; Texter, J. *Prog. Polym. Sci.* **2009**, *34*, 431. (b) Stepniak, I.; Andrzejewska, E. *Electrochim. Acta* **2009**, *54*, 5660. (c) Ueki, T.; Watanabe, M. *Macromolecules* **2008**, *41*, 3739. (d) He, Y.; Boswell, P. G.; Bühlmann, P.; Lodge, T. P. *J. Phys. Chem. B* **2007**, *111*, 4645. (e) Yeon, S. H.; Kim, K. S.; Choi, S.; Cha, J. H.; Lee, H. J. *J. Phys. Chem. B* **2005**, *109*, 17928.
- (5) (a) Jana, S.; Parthiban, A.; Chai, C. L. L. *Chem. Commun.* **2010**, 46, 1488. (b) Mudring, A. V. *Aus. J. Chem.* **2010**, *63*, 544. (c) Tu, T.; Bao, X.; Assenmacher, W.; Peterlik, H.; Daniels, J.; Dötz, K. H. *Chem.—Eur. J.* **2009**, *15*, 1853. (d) Sakai, H.; Saitoh, T.; Endo, T.; Tsuchiya, K.; Sakai, K.; Abe, M. *Langmuir* **2009**, *25*, 2601. (e) Puigmartí-Luis, J.; Laukhin, V.; del Pino, A. P.; Vidal-Gancedo, J.; Rovira, C.; Laukhina, E.; Amabilino, D. B. *Angew. Chem., Int. Ed.* **2007**, *46*, 238. (f) Liu, X. Y. *Top. Curr. Chem.* **2005**, *256*, 1. (g) Ikeda, A.; Sonoda, K.; Ayabe, M.; Tamaru, S.; Nakashima, T.; Kimizuka, N.; Shinkai, S. *Chem. Lett.* **2001**, 1154.
- (6) (a) Ueno, K.; Hata, K.; Katakabe, T.; Kondoh, M.; Watanabe, M. *J. Phys. Chem. B* **2008**, *112*, 9013. (b) Ueno, K.; Inaba, A.; Sano, Y.; Kondoh, M.; Watanabe, M. *Chem. Commun.* **2009**, 3603. (c) Park, C. L.; Jee, A. Y.; Lee, M.; Lee, S. *Chem. Commun.* **2009**, 5576. (d) Ueno, K.; Imaizumi, S.; Hata, K.; Watanabe, M. *Langmuir* **2009**, *25*, 825.
- (7) (a) Néeuze, M. A.; Bideau, J. L.; Gaveau, P.; Bellayer, S.; Vioux, A. *Chem. Mater.* **2006**, *18*, 3931.
- (8) (a) Fukushima, T.; Kosaka, A.; Ishimura, Y.; Yamamoto, T.; Takigawa, T.; Ishii, N.; Aida, T. *Science* **2003**, *300*, 2072. (b) Fukushima, T.; Aida, T. *Chem.—Eur. J.* **2007**, *13*, 5048. (c) Wang, J.; Chu, H.; Li, Y. *ACS Nano* **2008**, *2*, 2540.
- (9) (a) Welton, T. *Chem. Rev.* **1999**, *99*, 2071. (b) Torimoto, T.; Tsuda, T.; Okazaki, K.; Kuwabata, S. *Adv. Mater.* **2010**, *22*, 1196.
- (10) (a) Papagerorgiou, N.; Athanassov, Y.; Armand, M.; Bonhöite, P. H.; Pettersson, P.; Azamand, A.; Grätzel, M. *J. Electrochem. Soc.* **1996**, *143*, 3099. (b) Torimoto, T.; Tsuda, T.; Okazaki, K.; Kuwabata, S. *Adv. Mater.* **2010**, *22*, 1196. (d) Cai, N.; Zhang, J.; Zhou, D.; Yi, Z.; Guo, J.; Wang, P. *J. Phys. Chem. C* **2009**, *113*, 4215. (c) Yamanaka, N.; Kawano, R.; Kubo, W.; Kitamura, T.; Wada, Y.; Watanabe, M.; Yanagida, S. *Chem. Commun.* **2005**, 740.
- (11) (a) Shin, J. H.; Henderson, W. A.; Passerini, S. *Electrochem. Commun.* **2003**, *5*, 1016. (b) Sirisopanaporn, C.; Fericola, A.; Scrosati, B. *J. Power Sources* **2009**, *186*, 490. (c) Fericola, A.; Weise, F. C.; Greenbaum, S. G.; Kagimoto, J.; Scrosati, B.; Soletto, A. *J. Electrochem. Soc.* **2009**, *156*, A514. (d) Chew, S. Y.; Sun, J.; Wang, J.; Liu, H.; Forsyth, M.; MacFarlane, D. R. *Electrochim. Acta* **2008**, *53*, 6460.
- (12) (a) Brazier, A.; Appetecchi, G. B.; Passerini, S.; Vuk, A. S.; Orel, B.; Donsanti, F.; Decker, F. *Electrochim. Acta* **2007**, *52*, 4792. (b) Marcilla, R.; Alcaide, F.; Sardon, H.; Pomposo, J. A.; Pozo-Gonzalo, C.; Mecerreyes, D. *Electrochem. Commun.* **2006**, *8*, 482.
- (13) (a) Lauw, Y.; Horne, M. D.; Rodopoulos, T.; Nelson, A.; Leermakers, F. A. M. *J. Phys. Chem. B* **2010**, *114*, 11149. (b) Wei, D.; Ng, T. W. *Electrochem. Commun.* **2009**, *11*, 1996. (c) Simon, P.; Gogotsi, Y. *Nat. Mater.* **2008**, *7*, 845. (d) Balducci, A.; Dugas, R.; Taberna, P. L.; Simon, P.; Plée, D.; Mastragostino, M.; Passerini, S. *J. Power Sources* **2007**, *165*, 922.
- (14) (a) Ferraris, J.; Cowan, D. O.; Walatka, V.; Porlstein, J. H. *J. Am. Chem. Soc.* **1973**, *95*, 948. (b) Tomkiewicz, Y.; Torrance, J. B.; Scott, B. A.; Green, D. D. *J. Chem. Phys.* **1974**, *60*, 5111.
- (15) (a) Kistenmacher, T. J.; Phillips, T. E.; Cowan, D. O. *Acta Crystallogr. B* **1974**, *30*, 763. (b) Jerome, D. *Chem. Rev.* **2004**, *104*, 5565.
- (16) (a) Torrance, J. B.; Scott, B. A.; Welber, B.; Kaufman, F. B.; Seiden, P. E. *Phys. Rev. B* **1979**, *19*, 730. (b) Yakushi, K.; Ugawa, A.; Ojima, G.; Ida, T.; Tajima, H.; Kuroda, H.; Kato, R.; Kobayashi, H. *Mol. Cryst. Liq. Cryst.* **1990**, *181*, 217. (c) Kim, Y. H.; Jung, S. D.; Chung, M. A.; Song, K. D.; Cho, D. W. *Bull. Korean Chem. Soc.* **2008**, *29*, 948. (d) Xiao, J. C.; Yin, Z. Y.; Li, H.; Zhang, Q.; Boey, F.; Zhang, H.; Zhang, Q. C. *J. Am. Chem. Soc.* **2010**, *132*, 6926.
- (17) (a) Ouyang, J.; Yakushi, K.; Misaki, Y.; Tanaka, K. *J. Phys. Soc. Jpn.* **1998**, *67*, 3191. (b) Ouyang, J.; Dong, J.; Yakushi, K.; Takimiya, K.; Otsubo, T. *J. Phys. Soc. Jpn.* **1999**, *68*, 3708.
- (18) (a) Bozio, R.; Girlando, A.; Pecile, D. *Chem. Phys. Lett.* **1977**, *52*, 503. (b) Girlando, A.; Marzola, F.; Pecile, C.; Torrance, J. B. *J. Chem. Phys.* **1983**, *79*, 1075.
- (19) (a) Bozio, R.; Zanon, I.; Girlando, A.; Pecile, C. *J. Chem. Phys.* **1979**, *71*, 2282. (b) Van Duyne, R. P.; Cape, T. W.; Suchanski, M. R.; Siedle, A. R. *J. Phys. Chem.* **1986**, *90*, 739. (c) Ouyang, J.; Yakushi, K.; Misaki, Y.; Tanaka, K. *Phys. Rev. B* **2001**, *63*, 054301. (d) Ouyang, J.; Yakushi, K.; Kinoshita, T.; Nanbu, N.; Aoyagi, M.; Misaki, Y.; Tanaka, K. *Spectrochim. Acta, Part A* **2002**, *58*, 1643. (e) Yakushi, K.; Yamamoto, K.; Simonyan, M.; Ouyang, J.; Nakano, C.; Misaki, Y.; Tanaka, K. *Phys. Rev. B* **2002**, *66*, 235102.
- (20) Alves, A.; Molinari, A. S.; Xie, H.; Morpurgo, A. F. *Nat. Mater.* **2008**, *7*, 574.
- (21) (a) Chappell, J. S.; Bloch, A. N.; Bryden, W. A.; Maxfield, M.; Poehler, T. O.; Cowan, D. O. *J. Am. Chem. Soc.* **1981**, *103*, 2442.
- (22) (a) Chen, T. H.; Schechtman, B. H. *Thin Solid Films* **1975**, *30*, 173. (b) Vollmann, W.; Berger, W.; Hamann, C.; Libera, L. *Thin Solid Films* **1984**, *111*, 7.
- (23) Kistenmacher, T. J.; Phillips, T. E.; Cowan, D. O. *Acta Crystallogr. B* **1974**, *30*, 763.

(23) (a) Bag, B. G.; Maity, G. C.; Dinda, S. K. *Org. Lett.* **2006**, 8, 5457. (b) Rizkov, D.; Gun, J.; Lev, O.; Sicsic, R.; Melman, A. *Langmuir* **2005**, 21, 12130. (c) Das, R. K.; Banerjee, S.; Raffy, G.; Guerzo, A. D.; Desvergne, J. P.; Maitra, U. *J. Mater. Chem.* **2010**, 20, 7227.

(24) (a) Chiappe, C.; Malvalde, M.; Pomelli, C. S. *Pure Appl. Chem.* **2009**, 81, 767. (b) Ahosseini, A.; Scurto, A. M. *Int. J. Thermophys.* **2007**, 29, 1222.

(25) (a) Gale, R. J.; Osteroung, R. A. *Inorg. Chem.* **1979**, 18, 1603. (b) Tokuda, H.; Hayamizu, K.; Ishii, K.; Susan, A. B. H.; Watanabe, M. *J. Phys. Chem. B* **2005**, 109, 6103. (c) Shimomura, T.; Fujii, K.; Takamuku, T. *Phys. Chem. Chem. Phys.* **2010**, 12, 12316.

(26) (a) Froba, A. P.; Kremer, H.; Leipertz, A. *J. Phys. Chem. B* **2008**, 12, 12420. (b) Wang, P.; Zakeeruddin, S. M.; Humphry-Baker, R.; Gratzel, M. *Chem. Mater.* **2004**, 16, 2694. (c) Fei, Z.; Kuang, D.; Zhao, D.; Klein, C.; Ang, W. H.; Zakeeruddin, S. M.; Gratzel, M.; Dyson, P. J. *Inorg. Chem.* **2006**, 45, 10407. (d) Zhang, Z. X.; Gao, X. H.; Yang, L. *Chin. Sci. Bull.* **2005**, 50, 2005. (e) Del Sesto, R. E.; Corley, C.; Robertson, A.; Wilkes, J. S. *J. Organomet. Chem.* **2005**, 690, 2536.

(27) (a) Hill, B. S.; Scolari, C. A.; Wilson, G. S. *Philos. Trans. R. Soc. A* **1990**, 333, 63. (b) Cano, M.; Palenzuela, B.; Rodriguez-Amaro, R. *Electroanalysis* **2006**, 18, 1068.